Receptors and Channels, 9: 387–396, 2003
Copyright © Taylor & Francis Inc.
ISSN: 1060-6823 print / 1543-5334 online
DOI: 10.1080/10606820390257533

Taylor & Francis
healthsciences

Biophysical Properties of Kv3.1 Channels in SH-SY5Y Human Neuroblastoma Cells

P. Friederich
Universitätsklinik für Anästhesiologie, University of Hamburg, Hamburg, FRG

J. P. Dilger
Departments of Anesthesiology and Physiology and Biophysics, University at Stony Brook, Stony Brook, New York, USA

D. Isbrandt, K. Sauter, and O. Pongs
Institut für Neurale Signalverarbeitung, Zentrum für Molekulare Neurobiologie, University of Hamburg, Hamburg, FRG

B. W. Urban
Klinik für Anästhesiologie und spezielle Intensivmedizin, University of Bonn, Bonn, FRG, and Departments of Anesthesiology and Physiology, Weill Medical College of Cornell University, New York, New York, USA

Biophysical properties of delayed rectifier K channels in the human neuroblastoma SH-SY5Y were established using patch clamp recordings. The whole cell K^+ conductance activated at membrane potentials positive to −20 mV. The midpoint of current activation was 9.6 ± 5.1 mV, the equivalent charge was 3.7 ± .6. Whole-cell currents inactivated slightly with time constants of 700 ms and 5 s. The K^+ currents were sensitive to micromolar concentrations of TEA and 4-aminopyridine. RT-PCR experiments amplified a cDNA fragment specific for human Kv3.1 channels. Activation gating parameters in outside-out patches were shifted by ∼14 mV in the hyperpolarizing direction.

Keywords Gating, Patch-Clamp, Potassium Channel, Shaw

The human neuroblastoma cell-line SH-SY5Y expresses a variety of ion channels, including delayed rectifier K^+ channels, and it is widely used for laboratory studies (Seward and Henderson 1990; Reeve et al. 1991; Forsythe et al. 1992; Brown et al. 1994; Arcangeli et al. 1995; Meyer and Heinemann 1998). The biophysical and pharmacological properties of these K^+ channels have only been partially characterized (Reeve et al. 1991; Forsythe et al. 1992; Johannson et al. 1996; Tosetti et al. 1998), and their molecular identity is unknown. We have previously shown, using whole cell patch-clamp recording, that inhibition of delayed rectifier K^+ currents in SH-SY5Y cells by general anaesthetics, correlates with plasma concentrations of these drugs during anaesthesia (Friederich and Urban 1999; Friederich et al. 2001). Characterizing anaesthetic drug effects on these ion channels may, therefore, help to elucidate molecular mechanisms involved in the pharmacological action of anaesthetic agents. In view of these pharmacological results, and in view of the common use of SH-SY5Y cells in K^+ channel studies, it would be desirable to further characterize the biophysical and pharmacological properties of delayed rectifier K^+ channels in human neuroblastoma SH-SY5Y cells. For this purpose, we used the whole cell patch clamp configuration, as well as the reverse-transcription polymerase chain reaction (RT-PCR) and sequencing analysis, to identify the K^+ channel subtypes predominantly present in SH-SY5Y cells.

As outlined above, K^+ channels in SH-SY5Y cells may constitute a biophysical model for the study of molecular drug effects of anaesthetic agents. However, the analysis of the

Received April 2003; accepted September 2003.

This work was supported by grants from the Medical Faculty of Bonn University (BONFOR O-117.0005), the Deutsche Forschungsgemeinschaft, and Fonds der Chemischen Industrie. We are grateful to Z. Dorner for skillfully maintaining the cell culture and D. Clausen for excellent graphical assistance.

Address correspondence to P. Friederich, Universitätsklinik für Anästhesiologie, University of Hamburg, Martinistr. 52, 20251 Hamburg, FRG. E-mail: patrick.friederich@zmnh.uni-hamburg.de

magnitude and kinetics of drug action may be confounded by cell geometry and current amplitude. Space clamp and series resistance compensation are sometimes difficult to achieve in whole cell patch-clamp recordings of neurones. These problems can be overcome by studying excised patches. Another advantage of excised patches is that they allow for controlled, rapid changes of the bathing solution. This is an important prerequisite for studying the kinetics of drug actions on ion channels (Dilger et al. 1997). However, patch excision can also introduce artifacts. There is extensive evidence in the Na^+channel literature that channel gating parameters are affected by patch excision (Fenwick et al. 1982; Cachelin et al. 1983; Fernandez et al. 1984; Nagy et al. 1983; Kunze et al. 1985; Aldrich and Stevens 1987; Goldmann 1995). This has been demonstrated for Na^+ channels in various preparations, including neuroblastoma cells (Nagy et al. 1983; Aldrich and Stevens 1987; Goldmann 1995). To our knowledge, a similar comparison of whole cell and excised patch recordings has never been undertaken for delayed rectifier K^+ channels. Before any pharmacological study with excised patch-clamp recordings of delayed rectifier K^+ channels is performed, it is essential to compare the basic biophysical properties of these channels recorded with the whole cell and excised patch-clamp configurations first. The second aim of this investigation, therefore, was to compare the biophysical properties of delayed rectifier K^+ channels in human neuroblastoma SH-SY5Y cells in the whole cell and excised outside-out patch clamp configuration. Preliminary data of this study were presented as abstracts (Dilger et al. 1998; Friederich et al. 2000).

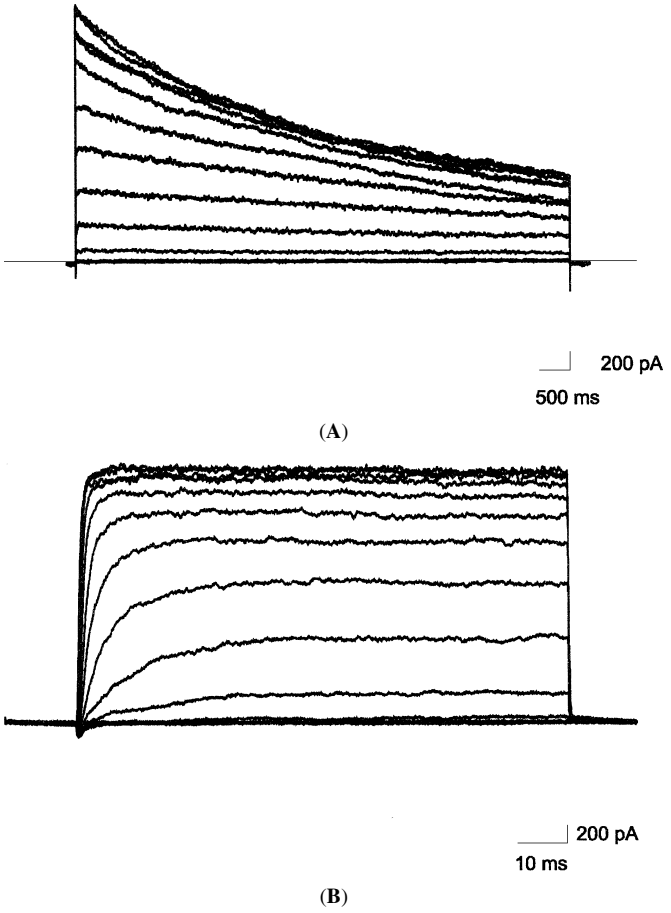

FIG. 1. Whole cell current traces at low (**A**) and high (**B**) time resolution. K^+ currents were evoked from a holding potential of −80 mV by depolarizing the cell membrane from −50 mV through +90 mV in 10 mV steps. The duration of the test depolarizations were 7.5 s and 84 ms respectively. Inactivation was not complete after a 7.5 s depolarization. The residual current amounted to 27 ± 6% of the peak current (n = 6, measured at +40 mV).

RESULTS

Whole Cell Electrophysiology

Outward delayed rectifier K^+ currents were evoked by depolarizing the cell membrane from a holding potential of −80 mV, to test potentials ranging from −50 mV to +90 mV in 10 mV steps (Figures 1A and 1B). The currents activated within a few milliseconds (Figures 1A and 1B), and inactivated on a time scale of seconds (Figure 1A). The K^+ currents saturated at membrane potentials more positive than +60 mV (Figure 2A). The saturating K^+ current level in SH-SY5Y cells was 2.95 ± .76 nA (n = 11). The average capacitance of the cells was 18 ± 4 pF (n = 11), so that the average current density was 170 ± 61 pA/pF (n = 11).

The K^+ conductance activated at membrane potentials more positive than −20 mV (Figure 2B). The membrane potential of half maximal activation was 9.6 ± 5.1 mV (n = 11); the equivalent charge was 3.65 ± 0.56 (n = 11). The K^+ conductance reached a plateau between +40 mV and +60 mV (Figure 2B) with a maximal amplitude of 19.4 ± 4.9 nS (n = 11). The deactivation time constant at −80 mV (measured in the presence of K_o = 40 mM) was 2.3 ± .9 ms (n = 4). The decline of the K^+ conductance at more depolarized potentials, a consequence of the saturating K^+ current, was quantified by calculating the ratio of the K^+ conductance at +80 mV to the maximal conductance (G_{80}/G_{max} = .89 ± .07, n = 11).

One possible cause for the decrease in conductance shown at large depolarizations is a block by intracellular Mg^{++}. This idea was tested by comparing whole cell current measurements made in the absence of Mg^{++} with those made in the presence of 4 mM Mg^{++} (Figure 2C, ATP was omitted from both of these intracellular solutions). The decrease in conductance was significantly less when Mg^{++} was omitted from the intracellular solution. For seven experiments in the absence of Mg^{++}, G_{80}/G_{max} = .94 ± .05; for seven experiments in the presence of 4 mM Mg^{++} (calculated free Mg^{++} 2.15 mM, under standard conditions the calculated free Mg^{++} was .91 mM), G_{80}/G_{max} = .86 ± .05 ($p < .05$, 2-tailed t-test). Because removal of Mg^{++} did not eliminate the decrease in conductance (Figure 2C), there must be an additional block. We did not further investigate the source of this block.

K current inactivation was not complete after a 7.5 s depolarization (Figure 1A). The residual current amounted to

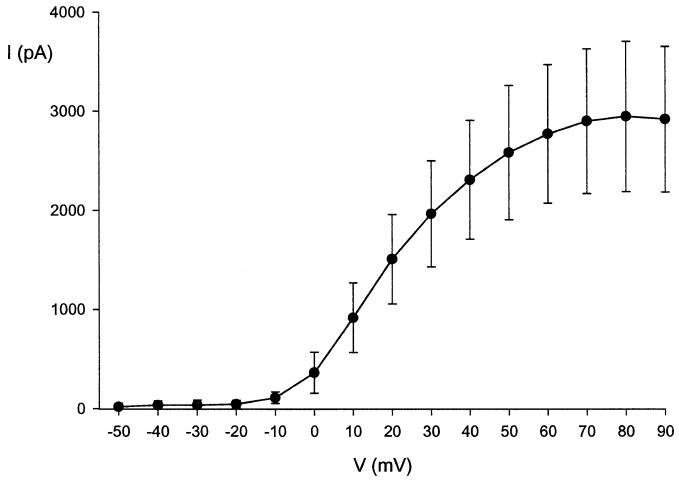

(**A**)

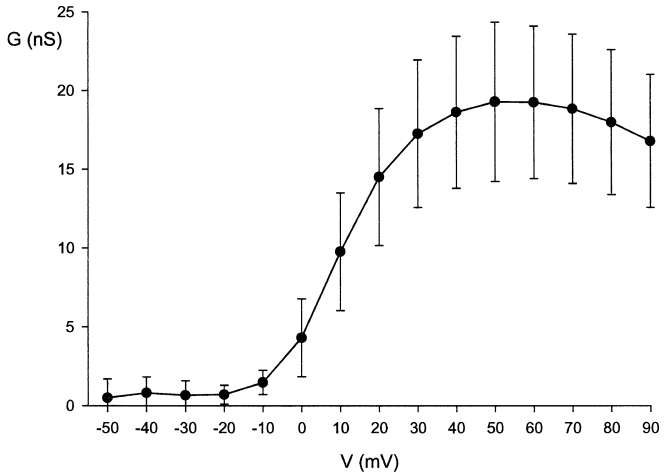

(**B**)

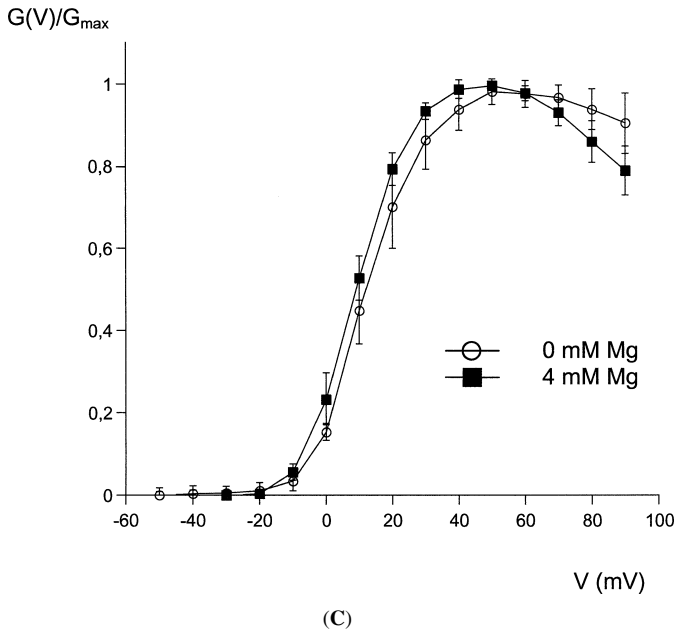

(**C**)

$27 \pm 6\%$ of the peak current (n = 6, measured at +40 mV). The rate of inactivation of the K^+ currents was voltage-independent (Figure 3A) and could be described as a bi-exponential decay with time constants of 700 ± 248 ms and 5060 ± 1260 ms (n = 6). The ratio of the amplitude of the fast component to the slow one was $.27 \pm .12$ (n = 6, measured at +40 mV). Steady-state inactivation (induced by 120 second depolarizations) was voltage-dependent (Figure 3B). The midpoint of the inactivation curve was −29 mV, and the equivalent charge was 2.4 ($n \leq 6$). Recovery from inactivation (Figure 3C) could be described as a single exponential process with a time constant of 2.6 s (n = 6).

Pharmacology

The pharmacological blockers tested on the K^+ currents in SH-SY5Y cells were all applied extracellularly. The K^+ currents were elicited by depolarizing the membrane potential from a holding potential of −80 mV to test potentials of 84 ms, duration ranging from −50 mV to +70 mV in 10 mV steps. Tetraethylammonium (TEA) produced a voltage-independent block with an IC_{50}-value of 105 μM (the maximal block was 93%, n = 16). Tetrapentylammonium (TPeA, n = 9) blocked the K^+ currents at lower concentrations than TEA. The block by TPeA was voltage-dependent with increasing inhibition at more depolarized potentials. At +70 mV, TPeA (10 μM) inhibited the K currents by $48 \pm 5\%$ (n = 4). The K^+ currents were also sensitive to micromolar concentrations of 4-aminopyridine (IC_{50}-value 35 μM, the maximal block was 93%, n = 7) and glibenclamide (IC_{50}-value 56 μM, n = 14). They were not affected by α-dendrotoxin at concentrations of .1 μM (n = 6).

Polymerase Chain Reaction and Sequence Analysis

The electrophysiological and pharmacological profile of the K^+ channels established in this study (Table 2) suggested that these channels belong to the Shaw, Kv3, subtype of K^+ channels (Gutman and Chandy 1995). Kv3 channels are the only Kv channels with a high threshold of activation and fast deactivation time constants, which are sensitive to micromolar concentrations of both tetraethylammonium and 4-AP; at the

FIG. 2. I-V (**A**) and G-V (**B**) curves: average from 11 whole cell experiments. Pulse protocol is described in Figure 1. The duration of the test-pulse was 84 ms. I-V and G-V curves were obtained by fitting every current trace to a two exponential time course (see Methods). The lines are drawn to connect the data points. (**C**) G-V curves comparing the effect of intracellular application of Mg^{2+} on G-V curves of high-threshold activating delayed rectifier potassium channels: average from 7 whole cell experiments. Pulse protocol is described in Figure 1. The duration of the test-pulse was 84 ms. The lines are drawn to connect the data points. The values of the activation midpoints derived by fitting the normalized conductance-voltage data with a Boltzmann function were $V_{mid} = 6.7 \pm 2.3$ mV for experiments with Mg^{2+} (4 mM) and $V_{mid} = 10.6 \pm 3.6$ mV for experiments without intracellular Mg^{2+} ($p < .05$). Currents were normalized to the maximum current within each individual experiment. The decrease in conductance at positive membrane potentials was significantly less when Mg^{++} was omitted from the intracellular solution.

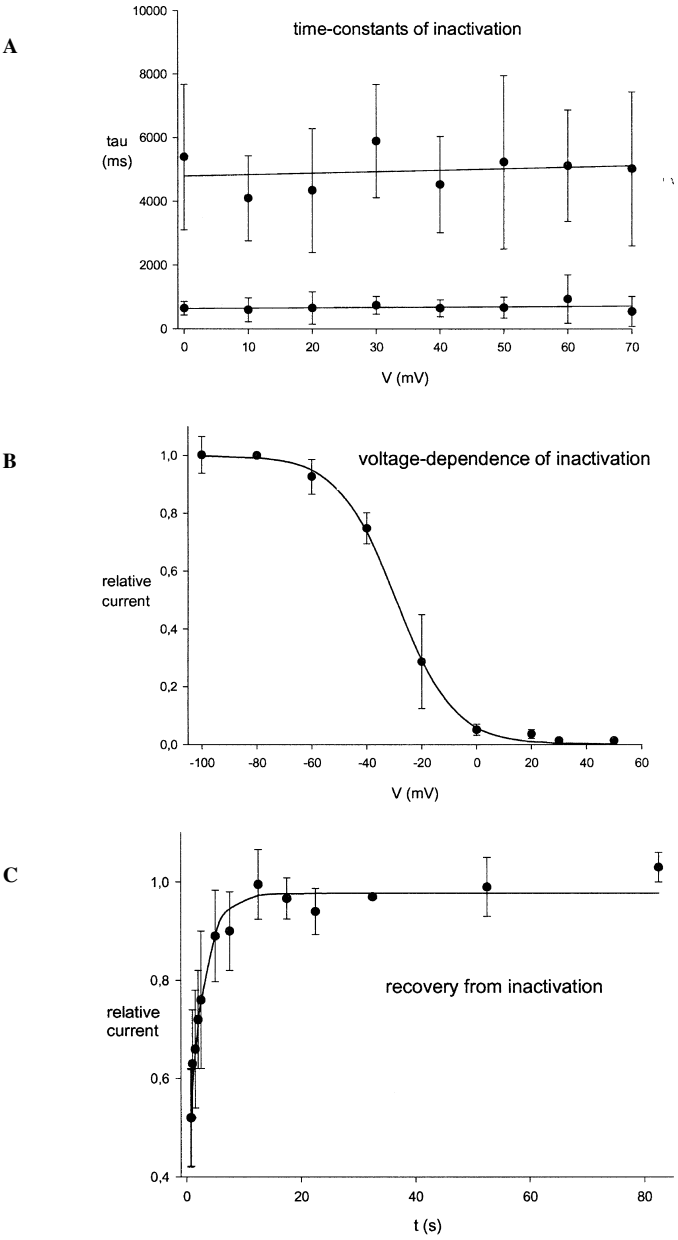

FIG. 3. (**A**) Inactivation proceeds with a double-exponential time course. Both time constants are independent of voltage. Double exponential functions were fit to the K^+ currents after they had reached their maximum. Currents were evoked by depolarizations of 7.5 s to the indicated membrane potentials (n = 6). (**B**) The voltage-dependence of steady-state inactivation induced by pre-pulses of a duration of 120 seconds to the indicated test-potentials from a holding potential of −80 mV (n = 3–6, at +30 mV n = 2 and at +50 mV n = 1). The extent of inactivation was elicited by subsequent depolarization to +40 mV. Inactivation was normalized to inactivation occurring at −80 mV. K^+ currents began to inactivate at membrane potentials more positive than −80 mV. (**C**) Recovery from inactivation occurs with a single time constant. K^+ currents were evoked from a holding potential of −80 mV by depolarizing the cell membrane to +40 mV. The test-pulse duration was 7.5 s. Recovery from inactivation was measured by a double-pulse protocol, where the interpulse duration varied between .7 s and 82.5 s. Recovery was expressed as the ratio of the maximal current amplitude, evoked by the second depolarization to the maximal current amplitude, evoked by the first depolarisation (n = 6).

same time, they are insensitive to α-dendrotoxin. The lack of N-type inactivation and the sensitivity to block by internal magnesium strongly points to the presence of Kv3.1 and/or Kv3.2 channels in SH-SY5Y cells (Gutman and Chandy 1995; Rudy et al. 1999). In order to strengthen the classification as Kv3.1 and/or Kv3.2 channels, we chose a molecular biological approach to support our electrophysiological and pharmacological results.

In order to confirm or exclude expression of Kv3.1 or Kv3.2 respectively in SH-SY5Y cells, we used reverse transcription polymerase chain reaction (RT-PCR) analyses. The cDNA sequence of human Kv3.1 was previously reported (Ried et al. 1993). Since the cDNA sequence of human Kv3.2 was not previously reported, it was established by a database search of the NCBI GenBank using rat Kv3.2 (Luneau et al. 1991) as a template and deposited in the database (accession number AY 118169). Both Kv3.1 and Kv3.2 cDNAs were used in a database search of the human genome to identify the first exon-intron border in the respective KCNC gene in order to design PCR assays with products spanning the border between exon 1 and 2 (please see Methods). The sensitivity and specificity of the PCR assays, which are close to an ideal PCR reaction, was determined by establishing standard curves using real-time quantitative PCR (please see Methods) and plasmid standards containing partial human Kv3.1 or Kv3.2 cDNAs respectively (please see Methods). We used the Kv3.1 or Kv3.2-specific PCR reactions to examine cDNA generated from reverse transcribed total RNA isolated from SH-SY5Y cells, or as a control, from human frontal cortex (Figure 4). As expected, both Kv3.1 and Kv3.2-specific fragments were amplified from human cortex. However, when we analyzed cDNA from SH-SY5Y cells, we were only able to detect Kv3.1-specific mRNA, but not Kv3.2-specific mRNA (Figure 4). Sequencing of the cDNA amplified with Kv3.1 specific primers, yielded the same nucleotide sequence as previously reported for Kv3.1 channels (Ried et al. 1993). Experiments repeated with independently isolated and reverse transcribed SH-SY5Y cDNA, as well as the use of additional Kv3.2-specific PCR primer pairs, yielded the same result (data not shown). These results, together with the previous findings from our electrophysiological and pharmacological experiments, demonstrate that SH-SY5Y cells functionally express Kv3.1, but not Kv3.2 channels.

Comparison of Whole Cell and Outside-Out Patch Currents

Figure 5 compares the K^+ currents shown in a whole cell with those shown in an outside-out patch taken from that cell. A small, quickly inactivating inward Na^+ current is shown in both the whole cell and outside-out patch currents. The outward K^+ currents exhibit a similar time course in both whole cell and outside-out patches, but the voltage sensitivity is shifted (arrows denote current resulting from depolarization to 0 mV). This shift is apparent in Figure 6, where the conductance-voltage curves

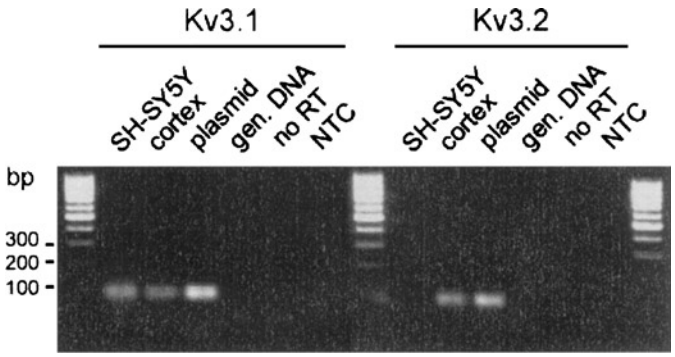

FIG. 4. Detection of Kv3.1-specific transcripts in cDNA from SH-SY5Y cells. RT-PCR amplification of a 71-bp DNA fragment, using Kv3.1-specific primers, indicates absence or presence of Kv3.1 sequences in the template material. A respective DNA fragment was amplified from SH-SY5Y total RNA (lane 1), from human frontal cortex total RNA (lane 2), and from Kv3.1 plasmid DNA (lane 3). The band was absent in control reactions, in which human genomic DNA (lane 4), SH-SY5Y total RNA without reverse transcription (lane 5), or water (NTC, lane 6) were used as templates. A Kv3.2-specific RT-PCR failed to detect Kv3.2 transcripts in cDNA from SH-SY5Y cells (lane 7). However, control reactions with human frontal cortex cDNA (lane 8) and Kv3.2 plasmid DNA (lane 9) yielded the correct fragment and proved the sensitivity of the reaction. Again, no Kv3.2-specific PCR-fragment could be detected in the negative controls performed similar to Kv3.1 (human genomic DNA lane 10, SH-SY5Y total RNA without reverse transcription lane 11, water lane 12).

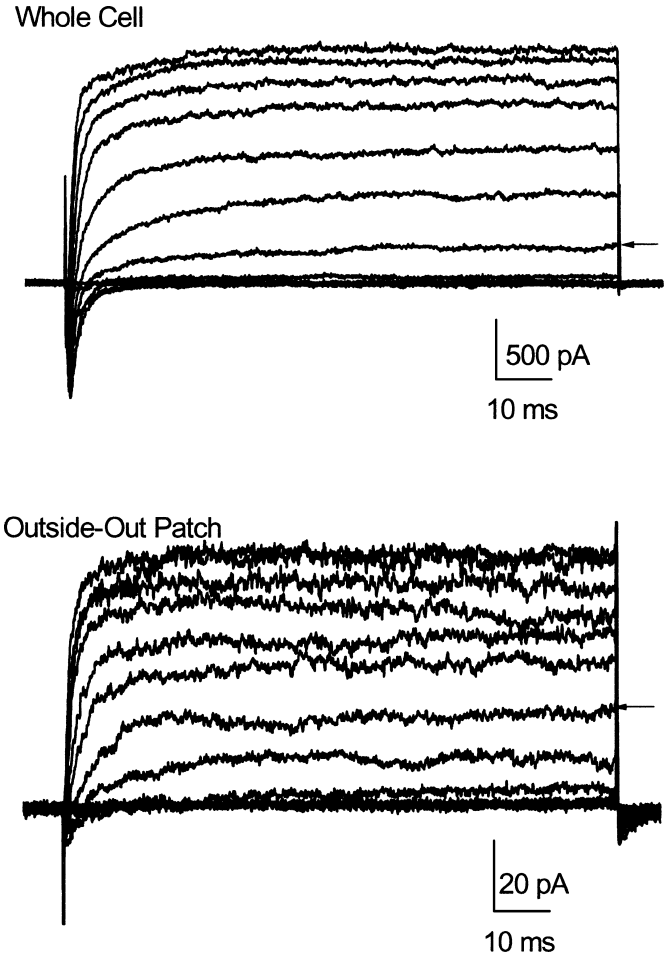

FIG. 5. Whole cell currents and currents from an outside-out patch from the same cell (E0210). P/4 leak subtraction was used. Holding potential −80 mV, 100 ms depolarizations to −50 through +60 mV in 10 mV steps. Arrows indicate current at a depolarization of 0 mV. The presence of tail currents in the outside-out patch current in Figure 5 (but, not observed in all patches) suggests that patch excision may have produced a depolarizing shift in the K^+ reversal potential. The shift in the activation midpoint, however, is in the hyperpolarizing direction. Thus, changes in K^+ reversal potential cannot account for the shift in the voltage dependence of the current following patch excision.

for both sets of currents are shown. The conductance midpoint of the outside-out patch currents in this cell is shifted 11 mV in the hyperpolarizing direction, compared to that of the whole cell. In addition, the conductance-voltage curve is less steep for the outside-out patch. A comparison of eight paired whole-cell and outside-out patch experiments is shown in Table 1. There is a significant difference between whole cell and outside-out patch K^+ currents in the midpoint (V_{mid} is shifted 14 mV towards hyperpolarized potentials), but not in the effective charge of the conductance-voltage curves.

The shift in voltage-sensitivity of the currents is also shown in the voltage-dependence of the activation time constant of the K^+ currents. Figure 7 summarizes the results of eight experiments, in which measurements were made on both whole cell currents and currents from an outside-out patch excised from the same cell. The activation time constant becomes faster with increasing depolarizations in both recording modes. However, the time constants are shifted 12 mV in the hyperpolarizing direction for outside-out currents, compared to whole cell currents (Figure 7).

TABLE 1

Comparison of the voltage sensitivity of K^+ currents in SH-SY5Y cells obtained under 8 paired whole-cell and outside-out patch recordings; p values are calculated using a 2-tailed, paired t-test

	V_{mid} (mV)	z_a	G_{max} (nS)
Whole cell	8.1 ± 3.3	4.1 ± 0.7	10.6 ± 3.7
Outside-out patch	-5.8 ± 6.7	2.9 ± 1.6	0.36 ± 0.29
p value	0.001	0.12	0.0001

DISCUSSION

Identification of Kv Channels

The voltage-dependent K^+ channels described in our study activate at high voltages with a positive activation midpoint. They exhibit C-type inactivation. These channels are highly sensitive to both TEA and 4-AP, and are insensitive to α-dendrotoxin. All of these properties are typical for Shaw-like Kv3 channels (Grissmer et al. 1994; Gutman and Chandy 1995; Rudy et al. 1999). The voltage-dependent K^+ channels in our study show inward rectification at positive potentials induced by internal

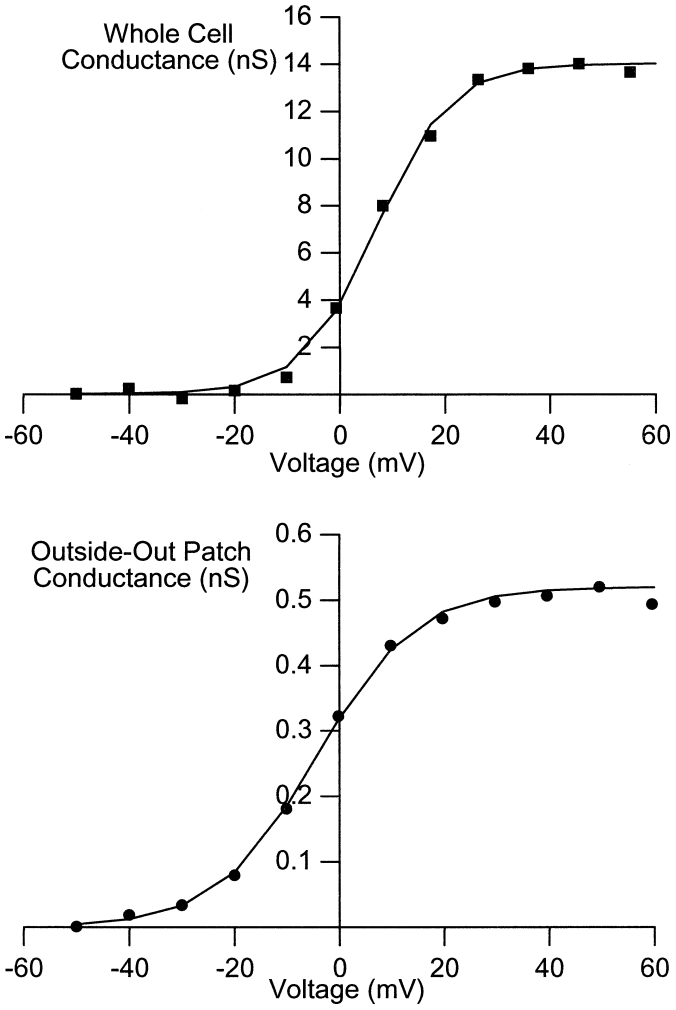

FIG. 6. Conductance voltage curves derived from the whole cell and outside-out patch experiments in Figure 5. The curves are fit to Equation 1 using the following parameters: whole cell: $V_{mid} = 6.9$ mV, $z_a = 3.7$; outside-out patch: $V_{mid} = -4.4$ mV, $z_a = 2.7$. When calculating V_{mid} with a reversal potential corrected by the calculated difference in driving force (20 mV) $V_{mid} = -7.2$ mV.

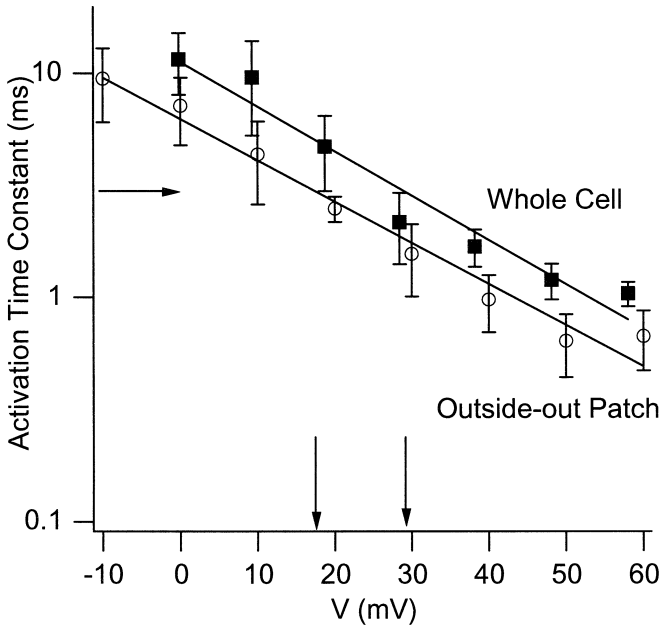

FIG. 7. A comparison of the activation kinetics of K^+ channels measured in whole-cell and outside-out patches. Results from 8 paired experiments. The slopes of the linear regressions give the voltage needed for an e-fold change in activation time constant: 51 mV for whole-cell and 54 mV for outside-out patch currents. The arrows indicate the voltage at which the activation time constant is 3 ms; 29 mV, for whole-cell and 17 mV for outside-out patch currents.

magnesium, a property that has been previously reported for rat Kv3.1 and Kv3.2 channels (Rettig et al. 1992; Harris and Isacoff 1996). In contrast to other Shaw-like channels, Kv3.1 and Kv3.2 do not exhibit N-type inactivation. N-type inactivation in Kv3 channels is introduced by the N-terminus of these ion channels, resulting in inactivation time constants in the range of 10 ms (Velasco et al. 1998). Kv3.1 and Kv3.2 inactivate with time constants of at least 50 times slower than described for N-type inactivation. Furthermore, C-type inactivation has been characterized in Kv3 channels cloned from rat brain (Marom et al. 1993). These experimental observations were the rationale for focusing on Kv3.1 and Kv3.2 in RT-PCR and sequencing experiments, in our study.

RT-PCR experiments with Kv3.1 specific primer, but not with Kv3.2 specific primer, amplified a cDNA fragment of 71 bp from SH-SY5Y cells. Two independent positive controls for Kv3.1, as well as Kv3.2, confirmed the specificity of the PCR reaction. Furthermore, the sensitivity of the RT-PCR assays was established in standard-curve reactions using real-time quantitative PCR. The templates were plasmids containing partial cDNAs for Kv3.1 or Kv3.2, respectively. The reactions showed that both reactions were comparably sensitive and close to an ideal PCR reaction (please see Methods). Sequencing analysis of the cDNA, amplified with Kv3.1 specific primers, yielded a nucleotide sequence previously reported for Kv3.1 channels (Ried et al. 1993). In combination, our electrophysiological, pharmacological, and molecular biologic results, therefore, suggest the functional expression of Kv3.1 channels in human SH-SY5Y cells.

The biophysical and pharmacological characteristics of the voltage-dependent K^+ channels expressed in SH-SY5Y cells, as described in our study, share certain similarities with those reported by others, but also differ in several aspects of their characteristics (Reeve et al. 1991; Forsythe et al. 1992; Johannson et al. 1996; Tosetti et al. 1998; Meyer and Heinemann 1998). All studies describe delayed rectifier K^+ currents in SH-SY5Y that activate at highly depolarized membrane potentials. The activation midpoints, however, vary between 0 mV and 37 mV, and only Johannsson et al. (1996), who also used series resistance compensation, report a voltage-dependence of activation similar to ours.

Another similarity between the K^+ channels measured by Johansson et al. (1996) and those investigated in our study, is

the marked rectification of the K^+ currents at high membrane potentials (Figures 2A and 2B). In the study by Johansson et al. (1996), rectification could be eliminated by removing Na^+ from the electrode solution. Our electrode solution, however, did not contain Na^+, but 4 mM Mg^{++}. We found that removal of internal Mg^{++} reduced, but did not eliminate, rectification. Johansson et al. (1996) estimated the internal Na^+-concentrations in intact SH-SY5Y cells to be approximately 15 mM. It is, therefore, conceivable that the rectification of the K^+ channels at high membrane depolarization, persisting in our study after Mg^{++} removal, may be attributed to residual intracellular Na^+ ions.

There are also some inconsistencies in the pharmacological profiles of delayed rectifier K^+ channels in SH-SY5Y cells measured by various groups. Most strikingly, our results and the results of Reeve et al. (1992) and Forsythe et al. (1992) indicate that the K^+ channels in SH-SY5Y cells are inhibited by low concentrations of 4-AP, whereas Tosetti et al. (1998) reported no inhibition at concentrations as high as 5 mM.

The differences in biophysical, as well as pharmacological properties, may be explained by differing cell culture and experimental conditions. We note that series resistance compensation was used in some, but not all of the studies. Forsythe et al. used K-gluconate in some of their experiments, whereas KCl was used by Johansson and in our study. In our laboratory, retinoic acid was used to induce differentiation in SH-SY5Y cells. K^+ channel expression in SH-SY5Y cells is influenced by retinoic-acid in a complex way (Meyer and Heinemann 1998). Retinoic acid induces a downregulation of h-eag channels and an increase in the number of delayed rectifier channels (Meyer and Heinemann 1998). Differences in biophysical and pharmacological profiles of the K^+ channels may also suggest that despite their genetic stability (Perez-Polo et al. 1979) SH-SY5Y cells may have diversified over the decades, since their initial description (Biedler et al. 1973), and express a different set of delayed rectifier K^+ channels in different laboratories. In any case, SH-SY5Y cells, as established in our laboratory, predominantly express Kv channels exhibiting properties resembling cloned Kv3.1 channels (Table 2, Rudy et al. 1999). In view of the physiological significance of Kv3.1 channels (Rudy 1999; Joho et al. 1999; Lau et al. 2000; Espinosa et al. 2001; Porcello et al. 2002), SH-SY5Y cells constitute a suitable cellular model to study Kv3.1 channels in a neuronal environment, as well as to investigate anaesthetic action on these important ion channels.

Whole Cell Versus Outside-Out Recordings

It has been known, since the early days of patch clamping, that patch excision may cause changes in the gating properties of Na^+ channels (Fenwick et al. 1982; Cachelin et al. 1983; Nagy et al. 1983; Fernandez et al. 1984; Kunze et al. 1985; Aldrich

TABLE 2
Properties of Kv3.1 channels in different preparations

	SH-SY5Y (This study)	NIH3T3 (Kanemasa)	L929 (Grissmer)	HEK 293 (Critz)	Oocytes (Yokoyama)	Oocytes (Kirsch)	Oocytes (Aiyar)	Oocytes (Rettig)	Oocytes (Grissmer)
Species	Human	Rat	Mouse	Rat	Mouse/rat	Mouse/rat	Mouse	Rat	Mouse
Activation									
Threshold (mV)	−20	−10	−10	−20	−10	−20			−30
Vmid (mV)	8.1	35.7	16	18		12	7.2	18.7	−1–16
Vsteep	6.1	20.8	8.7			7	12.8	9.7	9–11
Tau (ms)	1–10	Faster than oocyte			Fast				
Reversal (mV)	−79	−78							
Deactivation (ms)	2.5	1–3	1.4			1.3	1.8		1.4–2.6
Inactivation									
Tau (ms)	700/5000	3000–7000			Slow	7500	396	9822	
Vmidinac (mV)	−29								
Recovery tau (sec)	2.6								
Pharmacology (IC_{50}-values, μM)									
TEA	105	250	150	170	100	100	220	100	100
TpeA	10								
4-AP	35	200	29		600	80		250	180–600
Dtx	>1		>1					>100	
Gliben	56								

The first author is given in parentheses; Grissmer L292 refers to reference Grissmer et al. 1994. Vsteep means the number of millivolts needed to cause an e-fold change in open probability. The test drugs are abbreviated as follows: tetraethylammonium (TEA), tetrapentylammonium (TpeA), 4-aminopyridine (4-AP), α-dendrotoxin (Dtx), glibenclamide (Gliben).

and Stevens 1987). This has been seen in various preparations, including neuroblastoma cells. Our results show that a hyperpolarizing shift of gating parameters is not unique to Na^+ channels, and that remarkably quantitative similarities exist between Na^+ and K^+ channels in this respect. In mouse neuroblastoma N1E 115 cells, V_{mid} for Na^+ channel activation and inactivation is 12 mV more hyperpolarized in outside-out patches, compared to cell-attached patches (Nagy et al. 1993). In human neuroblastoma cells, we observed 12–14 mV hyperpolarizing shifts in K^+ channel activation and kinetics in outside-out patches, compared to whole-cell recordings.

Voltage-clamp problems may, in principle, account for the observed translation of gating parameters along the voltage axis. Total voltage clamp of the membrane would be achieved only in the outside-out patch clamp configuration. To minimize voltage clamp problems in our whole-cell experiments, however, we used 60% active compensation of the series resistance, and also calculated a corrected value of voltage for each current episode. The average difference between applied and corrected voltages close to V_0 was $-1.6 \pm .4$ mV. We consider it to be unlikely that the actual membrane potentials were an additional 12 mV hyperpolarized from our corrected values.

There are several other possible explanations for the observed gating shifts. Wendt et al. (1992) report that Na^+ channel gating remains stable during perforated patch, when compared to conventional whole cell patch clamp recordings. Also, Filipovic and Hayslett (1995) observed no alteration in channel gating, when using nystatin-perforated cell-attached patch as an alternative approach to excised inside-out patch. These studies imply that dilution of cytosolic components may cause the altered gating behavior of Na^+ and K^+ channels.

The interaction of Kvα and Kvβ subunits influences voltage-dependent gating of K^+ channels (Heinemann et al. 1996; Wang and Wu 1996; Accili et al. 1997). In contrast to our observations, a possible disruption of the interaction between alpha and beta subunits would probably result in a depolarising shift of the activation curve (Heinemann et al. 1996; Wang and Wu 1996; Accili et al. 1997). Interaction of Kv alpha and beta subunits with microfilaments may also influence K^+ channel function (Jing et al. 1999). In line with this hypothesis, a recent study by Shcherbatko et al. (1999) demonstrated that sodium channel gating is regulated by possible interaction with the cytoskeleton, and also through membrane mechanics. Presently, there are no reports that implicate a role of the cytoskeleton in the function of Kv3.1 channels. However, it is intriguing to speculate that interaction of the cytoskeleton with the cell membrane or directly with Kv3 channels may alter their voltage-dependent gating.

In conclusion, SH-SY5Y cells, as established in our laboratory, predominantly express Kv3.1 channels and constitute a model for the study of the properties and pharmacological alterations of these human K^+ channels in a native neuronal environment. Gating parameters are translated along the voltage-axis, when whole cell and outside-out patch-clamp measurements are compared. This shift is, thus, not unique to Na^+ channels and does not result from poor voltage-clamp conditions in whole-cell measurements. Whether or not the alteration of gating parameters affects the pharmacological properties of Kv3.1 channels remains to be studied.

MATERIALS AND METHODS

Cell Culture

SH-SY5Y cells were grown in a non-confluent monolayer using RPMI medium (Biochrom, Berlin, FRG) at 37°C in an atmosphere of 95% air and 5% CO_2. Growth medium contained 10% fetal calf serum, glutamine (2 mM), penicillin (100 U/ml), and streptomycin (100 μg/ml). Neuronal differentiation was induced by exposure to retinoic acid (10 μM) for 3–7 days. Treatment of these cells with retinoic acid resulted in a reduction in cell division and neurite extension (Pahlmann et al. 1984).

Whole-Cell Recordings

Voltage-sensitive outward currents were recorded at room temperature (22–25°C) with an EPC-7 amplifier (List Electronic, Darmstadt, FRG) and pClamp software Version 5.71 (Axon Instruments, Foster City, CA, USA), using the whole cell patch-clamp technique (Hamill et al. 1981). Patch electrodes with an input resistance between 1.8 and 3 MΩ were pulled from borosilicate glass capillary tubes (World Precision Instruments, Saratoga, Fl, USA), and were filled with the following internal solution (mM): KCl 115, $MgCl_2$ 1, MgATP 3, HEPES 10, EGTA 10, pH 7.2 (with KOH). The extracellular solution contained (mM): NaCl 135, KCl 4, $MgCl_2$ 1, $CaCl_2$ 2, Glucose 10, HEPES 10, pH 7.4 (with NaOH). Experiments with α-dendrotoxin were performed in the presence of .1% albumin. Series resistance was measured to be 4.6 ± 2.1 MΩ (mean ± SD, $n = 20$), and was actively compensated by 60%. The junction potential was measured to be 3.2 ± 0.9 mV (mean ± SD, $n = 5$) and was not corrected for. The holding potential was −80 mV, unless noted otherwise. The test potentials were rectangular pulses with a duration of 84 ms or 7.5 s, increasing from −50 mV to +90 mV in 10 mV steps with resting intervals of 1 s or 30 s at −80 mV, respectively. Currents were low pass filtered at 3 kHz, and sampled at 5 kHz. For graphical representation (Figure 1), current traces were digitally filtered at 1 kHz. Sodium and calcium currents have also been described in SH-SY5Y cells (Seward and Henderson 1990; Brown et al. 1994). Only a small percentage of the cells showed sodium currents. Moreover, at the holding potential of −80 mV, a substantial fraction of the sodium current was inactivated. Since sodium currents were generally small in size compared to the K^+ currents, they were not blocked. Any residual Na^+ current was inactivated by the depolarisation before the delayed rectifier K^+ channels were activated. Calcium channels were never shown with 2 mM extracellular $CaCl_2$. A P/4 leak subtraction protocol was used where noted, and performed from a holding potential of −80 mV.

Excised Patch Recordings

In experiments comparing whole-cell and excised patch currents, 1 or 2 families of whole-cell current-voltage traces were recorded before excising an outside-out patch. The capacitance compensation controls were re-adjusted. Four to five families of current-voltage traces were recorded in the outside-out mode. A P/4 leak subtraction protocol was used in both patch configurations. The families were averaged before performing the analysis.

Electrophysiological Data Analysis

The peak outward K^+ current in a trace was determined by fitting the current to a two exponential time course (activation and inactivation), and determining the maximal amplitude of the fit. This avoided the random error that would result from simply finding the maximum current (biased towards the highest noise level, especially for small, leak subtracted currents), and the systematic error that would result from using the maximum current at a specific time point for all voltages (the kinetics of activation are voltage-dependent). Peak currents were converted to conductances using the Nernst potential for K^+ (-85 mV for the standard K^+ concentration gradient; the measured reversal potential was -79 mV, $n = 2$), and voltage was corrected using the measured series resistance and compensation level (60%). The conductance-voltage data were fit to a Boltzmann function of the form:

$$G(V) = (G_{max} - G_{min})/(1 + \exp(-z_a F(V - V_{mid})/RT)) + G_{min} \quad [1]$$

where G_{max} and G_{min} are the maximum and minimum conductances measured for the data set; V_{mid} is the voltage corresponding to 50% of maximum conductance; z_a is the effective gating charge; and R, T, and F have their usual meanings. The fit routine used least-squares minimization to determine best-fit values of V_{mid} and z_a. To determine the degree of conductance inhibition at large depolarizations, a linear interpolation of the conductance data (between $+70$ and $+90$ mV before correction) was used to determine the conductance at $+80$ mV (corrected for series resistance), and the G_{80}/G_{max} ratio was calculated. Results are given as mean $\pm$ SD.

Reverse Transcription, Polymerase Chain Reaction, and Sequence Analysis

The presence of Kv3.1 and Kv3.2 mRNA in SH-SY5Y cells was established by RT-PCR and subsequent sequencing of the PCR-product. The sensitivity of the PCR reactions described below was quantified using SybrGreen (Applied Biosystems, Foster City, California, USA) real-time quantitative PCR on an ABI 7900HT (Applied Biosystems, Foster City, California, USA). Standard curves performed in triplicate using plasmid standards of Kv3.1 or Kv3.2 respectively confirmed the sensitivity of the PCR reaction and the absence of primer dimer formation. They verified the high reproducibility of the Kv3.1/Kv3.2 PCR assays, as well as the independence of amplification kinetics from the template concentration. This allowed the generation of Ct value standard curves (Kv3.1: $r = .997$, slope $= -3.6 \pm .026$, intercept $= 38.2 \pm .8$ ($n = 3$); Kv3.2: $r = .997$, slope $= -3.2 \pm .04$, intercept $= 37.4 \pm .7$ ($n = 3$)) for absolute quantification of plasmid standard Kv3.1 or Kv3.2 molecules. The mean slopes of -3.6 and -3.2 were close to the theoretical value of -3.32 ($-1/\log 2$) for a perfect PCR reaction that exactly doubles the number of template molecules with each cycle.

For reverse transcription, a reaction volume of 12 μl, containing 250 ng random primer (1μl, Gibco-BRL, Rockville, Maryland, USA), 1 μg total RNA (1μl), and distilled water, was heated to 70°C for 10 minutes. 5 × first strand buffer (4 μl, pH 8.3, Gibco-BRL, Rockville, Maryland, USA), .1 M DDT (2 μl, all from Gibco-BRL, Rockville, Maryland, USA), and 10 mM dNTP (1 μl, Amersham Pharmacia, Freiburg, FRG) were then added, and the reaction volume was incubated at 25°C for 10 minutes and at 42°C for 2 minutes. Superscript II RNAse H^- reverse transcriptase (1 μl, 200 units, Gibco-BRL, Rockville, Maryland, USA) was added, and the volume was incubated at 42°C for 50 minutes. The reaction was stopped by heating to 70°C for 15 minutes, and the cDNA was used as the template for the PCR.

For PCR amplification (ABI 7900HT), 50 μl of a solution containing $MgCl_2$ (1.5 mM), DMSO (5%), 10 × buffer (10 μl, Gibco-BRL, Rockville, Maryland, USA), dNTP mix (200 μM, Gibco-BRL, Rockville, Maryland, USA), TAQ-polymerase (2.5 units, Gibco-BRL, Rockville, Maryland, USA), cDNA (1 μl), Kv3.1 sense primer (5′-CGCTACGCG CGGTATGT-3′), and Kv3.1 antisense primer (5′-TCCAGGCAGAAGGTGGTGAT-3′) and Kv3.2 sense primer (5′-CTTCGAAGACCCCTACTCGT CC-3′) and Kv3.2 antisense primer (5′-AACCAGGATGAAGA-ATAAAGAAGC-3′) were added to a test tube (100 pmol, 0.5 μl each). The tubes were preheated for 5 minutes at 94°C, and were then subjected to 40 cycles of a two-step PCR consisting of denaturation at 94°C (30 seconds) and annealing/extension at 60°C (30 seconds). The SybrGreen standard curve PCRs were followed by a slow temperature ramp, yielding a melting curve. The PCR products were separated on a 2% agarose gel by electrophoresis (80–100 mV; Pharmacia LKB, Upsalla, Sweden) and visualised by ethidium bromide staining. The PCR products generated by the Kv3.1 or Kv3.2 primers span the intron between exon1 and exon2 of the KCNC1 or KCNC2 genes. The exon1/intron1 borders of the KCNC1 or KCNC2 genes were established by a blast search (Altschul et al. 1997) at the NCBI Genbank human genome database using the respective cDNA as a template (Genbank Accession numbers: Kv3.1: NM_004976; Kv3.2: AY118169). For KCNC1 (Kv3.1), the first exon/intron border is located between nucleotides 570 and 571 of the KCNC1 open reading frame. For KCNC2 (Kv3.2) the first exon/intron border is located between nucleotides 687 and 688 of the KCNC2 open reading frame. After purification, the PCR products were sequenced using the BIG DYE cycle

sequencing kit (Applied Biosystems, USA) and analyzed on an ABI 377 automated sequencer (Applied Biosystems, USA). As a positive control for Kv3.1, a fragment containing nt 192–697 of hKv3.1 was amplified from human cortex cDNA, subcloned to pCRII-Topo (Invitrogen, Groningen, The Netherlands), and verified by sequencing analysis. For Kv3.2, an EST clone containing a fragment of human Kv3.2 (Kv3.2: IMAGp998D15331, RZPD, Berlin, FRG) was verified by sequencing analysis and served as a positive control. Both positive controls served as standards in the above described PCR experiments.

REFERENCES

Accili, E. A., Kiehn, J., Yang, Q., Wang, Z., Brown, A. M., and Wible, B. A. 1997. *J. Biol. Chem.* 272:25824–25831.

Aiyar, J., Nguyen, A. N., Chandy, K. G., and Grissmer, S. 1994. *Biophys. J.* 67:2261–2264.

Aldrich, R. W., and Stevens, C. F. 1987. *J. Neurosci.* 7:418–431.

Altschul, S. F., Madden, T. L., Schaffer, A. A., Zhang, J., Zhang, Z., Miller, W., and Lipman, D. J. 1997. *Nucleic. Acids Res.* 25:3389–3403.

Arcangeli, A., Bianchi, L., Becchetti, A., Faravelli, L., Colonnello, M., Mini, E., Olivotto, M., and Wanke, E. 1995. *J. Physiol.* 489:455–471.

Biedler, J. L., Helson, L., and Spengler, B. A. 1973. *Cancer Research* 33:2643–2652.

Brown, N. A., Kemp, J. A., and Seabrook, G. A. 1994. *Br. J. Pharmacol.* 113:600–606.

Cachelin, A. B., De Peyer, J. E., Kokubun, S., and Reuter, H. 1983. *J. Physiol.* 340:389–401.

Chow, A., Erisir, A., Farb, C., Nadal, M. S., Ozaita, A., Lau, D., Welker, E., and Rudy, B. 1999. *J. Neurosci.* 19:9332–9345.

Cleveland, D. W., Fischer, S. G., Kirschner, M. W., and Laemmli, U. K. 1977. *J. Biol. Chem.* 252:1102–1106.

Critz, S. D., Wible, B. A., Lopez, H. S., and Brown, A. M. 1993. *J. Neurochem.* 60:1175–1178.

Dilger, J. P., Boguslavsky, R., Barann, M., Katz, T., and Vidal, A. M. 1997. *J. Gen. Physiol.* 109:401–414.

Dilger, J. P., Friederich, P., and Urban, B. W. 1998. *Soc. Neurosci. Abstract* 24:813–813.

Espinosa, F., McMahon, A., Chan, E., Wang, S., Ho, C. S., Heintz, N., and Joho, R. H. 2001. *J. Neurosci.* 21:6657–6665.

Fenwick, E. M., Marty, A., and Neher, E. 1982. *J. Physiol.* 331:599–635.

Fernandez, J. M., Fox, A. P., and Krasne, S. 1984. *J. Physiol.* 356:565–585.

Filipovic, D., and Hayslett, J. P. 1995. *J. Membr. Biol.* 148:79–82.

Forsythe, I. D., Lambert, D. G., Nahorski, S. R., and Linsdell, P. 1992. *Br. J. Pharmacol.* 107:207–214.

Friederich, P., and Urban, B. W. 1998. *Brain. Res. Mol. Brain Res.* 60:301–304.

Friederich, P., and Urban, B. W. 1999. *Anesthesiology* 91:1853–1860.

Friederich, P., Dilger, J. P., Pongs, O., and Urban, B. W. 2000. *Pflügers Arch. Eur. J. Physiol.* 439:R 427.

Friederich, P., Benzenberg, D., Trellakis, S., and Urban, B. W. 2001. *Anesthesiology* 95:954–958.

Goldman, L. 1995. *Biophys. J.* 69:2364–2368.

Grissmer, S., Ghanshani, S., Dethlefs, B., McPherson, J. D., Wasmuth, J. J., Gutman, G. A., Cahalan, M. D., and Chandy, K. G. 1992. *J. Biol. Chem.* 267:20971–20979

Grissmer, S., Nguyen, A. N., Aiyar, J., Hanson, D. C., Mather, R. J., Gutman, G. A., Karmilowicz, M. J., Auperin, D. D., and Chandy, G. 1994. *Mol. Pharmacol.* 45:1227–1234.

Gutman, K. G., and Chandy, G. A. 1995. Voltage-Gated K Channel Genes. In: Handbook of Receptors and Channels. Eds. North A, CRC Press LLC, Boca Raton, Florida, pp. 1–47.

Hamill, O. P., Marty, A., Neher, E., Sakmann, B., and Sigworth, F. J. 1981. *Pflügers Arch. Eur. J. Physiol.* 391:85–100.

Harris, R. E., and Isacoff, E. Y. 1996. *Biophys. J.* 71:209–219.

Heinemann, S. H., Rettig, J., Graack, H. R., and Pongs, O. 1996. *J. Physiol.* 493:625–633.

Hernandez-Pineda, R., Chow, A., Amarillo, Y., Moreno, H., Saganich, M., de Miera, E. V., Hernandez-Cruz, A., and Rudy, B. 1999. *J. Neurophysiol.* 82:1512–1528.

Jing, J., Chikvashvili, D., Singer-Lahat, D., Thornhill, W. B., Reuveny, E., and Lotan, I. 1999. *EMBO J.* 18:1245–1256.

Johansson, S., Sundgren, A. K., and Kahl, U. 1996. *Am. J. Physiol.* 270:C1131–1144.

Joho, R. H., Ho, C. S., and Marks, G. A. 1999. *J. Neurophysiol.* 82:1855–1864.

Kanemasa, T., Gan, L., Perney, T. M., Wang, L. Y., and Kaczmarek, L. K. 1995. *J. Neurophysiol.* 74:207–217.

Kirsch, G. E., Shieh, C. C., Drewe, J. A., Vener, D. F., and Brown, A. M. 1993. *Neuron.* 11:503–512.

Kunze, D. L., Lacerda, A. E., Wilson, D. L., and Brown, A. M. 1985. *J. Gen. Physiol.* 86:691–719.

Lau, D., Vega-Saenz, de Miera, E. C., Contreras, D., Ozaita, A., Harvey, M., Chow, A., Noebels J. L., Paylor, R., Morgan, J. I., Leonard, C. S., and Rudy, B. J. 2000. *J Neurosci.* 20:9071–9085.

Luneau, C., Wiedmann, R., Smith, J. S., and Williams, J. B. 1991. *FEBS Lett.* 288:163–167.

Marom, S., Goldstein, S. A., Kupper, J., and Levitan, I. B. 1993. *Receptors Channels* 1:81–88.

Meyer, R., and Heinemann, S. H. 1998. *J Physiol.* 508:49–56.

Nagy, K., Kiss, T., and Hof, D. 1983. *Pflügers Arch. Eur. J. Physiol.* 399:302–308.

Nakahira, K., Matos, M. F., and Trimmer, J. S. 1998. *J. Mol. Neurosci.* 11:199–208.

Pahlman, S., Ruusala, A. I., Abrahamsson, L., Mattsson, M. E., and Esscher, T. 1984. *Cell Differ.* 14:135–144.

Perez-Polo, J. R., Werbach-Perez, K., and Tiffany-Castiglioni, E. 1979. *Dev. Biol.* 71:341–355.

Porcello, D. M., Ho, C. S., Joho, R. H., and Huguenard J. R. 2002. *J. Neurophysiol.* 87:1303–1310.

Reeve, H. L., Vaughan, P. F. T., and Peers, C. 1992. *Neurosci. Lett.* 135: 37–40.

Rettig, J., Wunder, F., Stocker, M., Lichtinghagen, R., Mastiaux, F., Beckh, S., Kues, W., Pedarzani, P., Schroter, K. H., Ruppersberg, J. P., Veh, R. W., and Pongs, O. 1992. *EMBO J.* 11:2473–2486.

Ried, T., Rudy, B., Vega-Saenz, de Miera, E., Lau, D., Ward, D. C., and Sen, K. 1993. *Genomics* 15:405–411.

Rudy, B., Chow, A., Lau, D., Amarillo, Y., Ozaita, A., Saganich, M., Moreno, H., Nadal, M. S., Hernandez-Pineda, R., Hernandez-Cruz, A., Erisir, A., Leonard, C., and Vega-Saenz de Miera, E., Ann, N.Y. 1999. *Acad. Sci.* 868:304–343.

Seward, E. P., and Henderson, G. 1990. *Pflügers Arch. Eur. J. Physiol.* 417:223–230.

Shcherbatko, A., Ono, F., Mandel, G., and Brehm, P. 1999. *Biophys. J.* 77:1945–1959.

Tosetti, P., Taglietti, V., and Toselli, M. 1998. *J. Neurophysiol.* 79:648–658.

Veh, R. W., Lichtinghagen, R., Sewing, S., Wunder, F., Grumbach, I. M., and Pongs, O. 1995. *Eur. J. Neurosci.* 7:2189–205.

Velasco, I., Beck, E. J., and Covarrubias, M. 1998. *Neurobiology* 6:23–32.

Wang, J. W., and Wu, C. F. 1996. *Biophys. J.* 71:3167–3176.

Wendt, D. J., Starmer, C. F., and Grant, A. O. 1992. *Am. J. Physiol.* 263:C1234–1240.

Weiser, M., Vega-Saenz, de Miera, E., Kentros, C., Moreno, H., Franzen, L., Hillman, D., Baker, H., and Rudy, B. 1994. *J. Neurosci.* 14:949–972.

Yokoyama, S., Imoto, K., Kawamura, T., Higashida, H., Iwabe, N., Miyata, T., and Numa, S. 1989. *FEBS Lett.* 259:37–42.